Proceedings of the 16th European Turbomachinery Conference (ETC16)
Turbomachinery, Fluid Dynamics and Thermodynamics,
March 24-28, 2025, Hannover, Germany

# Fluid Topology Optimization of Film Cooling: a Design Exploration

[1,2]Francesco Montomoli, [1]Thomas W. Rees, [1]Stefano Furino, [1]Ruben Tomlin
[1]ToffeeX, London, UK
[2]Imperial College London, London, UK

**Abstract**

This paper presents a design exploration analysing the film cooling channels optimized using fluid topology optimization (FTO) that can be obtained via additive manufacturing. The primary objective is to identify the differences and similarities between these optimized designs and current solutions. The design region considered in this study includes the internal channel, the coolant exit hole, and the surface upstream of the cooled hole. Two baseline design domains are examined: a fan-shaped coolant duct, to evaluate whether FTO can enhance performance based on existing optimized designs, and a wider domain, to explore alternative solutions, allowing FTO to generate new geometries. To carry out this analysis the platform ToffeeX is used. The objective functions employed aim to minimize pressure losses while maximizing coolant coverage on the surface. The optimization process generated multiple configurations, which are more complex than standard designs. When FTO is applied to an existing shaped channel, multi-hole configurations are generated and the adiabatic effectiveness is increased. More interesting geometries emerged when allowing a wider design space. In this case, four main features often appeared: branching within the channel, multihole exits, steps before the holes and deep pockets on the side of the main hole (fed by the main channel). The observed performance improvements varied depending on free-stream turbulence level. Both the baseline and optimized geometries were tested under a wide range of operating conditions, with the optimized designs showing performance gains depending on the turbulence level of the free stream.

**Keywords**: film cooling, fluid topology optimization, additive manufacturing

## 1 Introduction

Engineers have raised the turbine inlet temperature to levels exceeding the melting point of the alloys used in blades. These extreme temperatures necessitate advanced cooling techniques [1]. Among these, film cooling has gained significant attention due to its ability to shield high-pressure turbine nozzles and rotors from hot gases by creating a protective layer of coolant.

The influence of coolant hole geometry on lateral adiabatic effectiveness was first studied by Goldstein et al. [2], who demonstrated the advantages of shaped holes over standard cylindrical holes. The key effect observed was a reduction in the momentum of the coolant perpendicular to the cooled wall, which minimized jet lift-off. Andreopulos and Rodi [3] later provided a detailed analysis of the flow structures causing coolant lift-off and reduced coverage, identifying a pair of counter-rotating vortices, known as "kidney vortices," as the primary cause of jet lift-off. These vortices are generated by the redistribution of the boundary layer within the coolant duct and push the coolant away from the surface through their interaction.

Various geometries have been proposed to mitigate these vortices, including cusp designs [4], laid-back shaped holes [5-7], among others. The common goal of these designs is to reduce the interaction of kidney vortices and minimize the coolant perpendicular momentum component, thus maximizing coolant effectiveness. As Gritsch et al. [7] demonstrated, these geometries minimize the vorticity component aligned with the free stream, enabling the cooling film to remain attached to the surface.

More recent strategies have modified the blade external surface to better distribute the coolant. Researchers such as Wu et al. [8] have proposed embedding coolant holes in shaped craters and trenches to improve coolant coverage, which has proven highly effective. The proposed designs can be achieved either by controlling the thermal barrier coating thickness or by shaping the surface before the coolant hole to form steps, domes, or other structures that enhance cooling efficiency. For instance, Oguntade et al. [9] introduced shaped trench cavities to improve film cooling, while Montomoli et al. [10] employed a double back-facing step over the coolant hole to increase lateral coverage, even for aggressive designs with large pitch-to-diameter ratios.

Many of these designs are based on the fundamental physics of kidney vortex interaction and engineering intuition and experience. However, manufacturability also plays a crucial role, as these channels are often created using lasers, which impose limitations on the geometries' angles and shapes. Recently, additive manufacturing has enabled the exploration of more intricate geometries, previously unimaginable. Despite the limitations of additive manufacturing, such as overhang angles and minimum feature sizes, it offers greater flexibility for complex designs. Snyder et al. [11] reviewed several high-performing shapes, such as consoles, crescents, oscillators, spirals, and tripods, which are now fully realizable through additive manufacturing.

Although significant progress has been made in developing optimal film cooling designs using additive techniques, the full potential of the design space enabled by additive manufacturing remains unexplored. One promising computational tool for designing components for additive manufacturing is topology optimization. Traditionally used for optimizing or reducing the weight of structural components, recent breakthroughs have demonstrated the applicability of topology optimization in thermo-fluid systems.

Fluid Topology Optimization (FTO) has gained recent attention. Dede et al. [12-13] used FTO code to a squared heat dissipator. In 2010, Yoon [14] used a similar approach for two dimensional problems. Matsumori et al. [15] introduced the method with conjugate heat transfer and in more recent



Paper ID: ETC2025-293

years, Marck and Privat [16] and Alexandersen et al. [17] introduced porosity-dependent thermal conductivity.
This paper aims to introduce and explore the performances of new geometries for optimal film cooling in gas turbines, generated using fluid topology optimization. While fluid topology optimization, as described by Raske et al. [18] and Pietropaoli et al. [19], has shown promise in developing high-performance geometries for cooling systems—primarily in single-fluid heat exchangers. Very recently the same platform used in this work has been applied to model fuel cells and two fluid heat exchangers [20-22]. This is the first time the method has been applied to film cooling.

**NOMENCLATURE**

| | |
|---|---|
| c | Heat capacity |
| $f_t$ | Objective function, temperature |
| p | Lateral pitch |
| s | Axial pitch |
| D | Film cooling diameter |
| M | Blowing ratio |
| T | Temperature |
| $T_{aw}$ | Adiabatic wall temperature |
| $T_m$ | Temperature hot gas |
| $T_c$ | Temperature coolant |
| x,y,z | Principal Cartesian Axis |
| $\gamma$ | Heat capacity ratio |
| $\rho$ | Density |
| $\eta$ | Adiabatic film cooling effectiveness |
| $\Omega$ | Volume |
| TU | Turbulent intensity |

## 2 Methodology

The fluid topology optimization (FTO) method employed in this study has been introduced and applied in previous publications [18-22] and used here. The performance of the optimized designs has been compared favorably with predictions obtained with other commercial software and experimental results, while it should not be considered a substitute for high fidelity simulation. In the present work the same formulation as in previous work has been used.
The film cooling designs presented in this work were obtained using the ToffeeX physics-driven design platform. Based primarily on fluid topology optimization, ToffeeX uses a finite volume method Reynolds-averaged Navier Stokes (RANS) method to solve the governing equations based on user defined boundary conditions. The solid field is represented in the fluid TO problem with a Brinkmann impermeability term. The mathematical formulation and the boundary conditions used can be found in detail in [18-22].
For the optimization, the solver controls the solid distribution in a fluid medium without a priori specification of the shape or implicit modelling. The optimal design is obtained by allowing each point of the design domain to switch between being either fluid or solid.
Multiobjective optimization is used. All specific objectives in ToffeeX are weighted against the pressure losses, defined as in [20] (1):

$$f_p = \int_\Gamma \left(p + \frac{1}{2}|v|^2\right) v.n \, d\Gamma \quad (1)$$

The integral of pressure losses is evaluated over the boundary of the domain and therefore the function is the difference in total pressure losses between inlet and outlet of the design space.
To generate the optimized cooling geometry, the solver requires a defined design domain within which it can solve the physical governing equations and generate the optimized geometry.
In this work, two design domains are used

1) shaped hole proposed by [7]
2) wider volume to explore more complex solutions.

This design domain delineates the volume where the FTO optimizer can make modifications; the solver cannot add volume outside this specified geometry. It is possible to fine tune the optimization in the design domain by specifying regions with specific constraints; this is done in a graphical user interface (GUI). By outlining volumes, multiple constraints can be applied, encompassing variations in fluid and solid properties (thermal conductivity, density, heat capacity etc), heat sources, and specific volumetric optimization targets like component weights, local thermal gradients, or maximum temperatures.
In addition, the geometry is optimized to manufacturing constraints, such as minimum passing area, minimum feature size, constraints on overhang angles (essential for additive manufacturing) etc. Although the geometry presented in this study was tailored for additive manufacturing, the solver can also optimize for alternative manufacturing methods like milling, stamping etc. In case of film cooling, only the external part of the hole can be optimized using milling constraint.
For the optimization of film cooling, two different objective functions have been explored independently, while minimizing pressure losses:

1) Maximization of heat transfer downstream the coolant injection (in case of perfect cooling, this would have allowed the maximum reduction of metal temperature)
2) Minimization of temperature downstream the coolant injection, from downstream edge to the exit (with a distance up to 0.2D from the cooled surface) allowing the generation of solid structures.

The minimization of temperature or the target temperature is achieved with an integral over the specific volume as in [20].
Minimization of temperature objective function (2):

$$f_t = \int_\Omega (\gamma \rho c T) \, d\Omega \quad (2)$$

where $\gamma$ is the solidity, $\rho$ is the fluid density and c is the specific heat capacity.

## 3 Film-cooling hole test case

The baseline geometry used for the current optimization is based on the shaped hole design proposed by the "Institut für Thermische Strömungsmaschinen" (ITS) at the University of Karlsruhe, as described by Gritsch et al. (2000) [7]. In the original design, the coolant duct and the main flow were two independent loops, which could be aligned either parallel or perpendicular to each other. In this study, the coolant channel

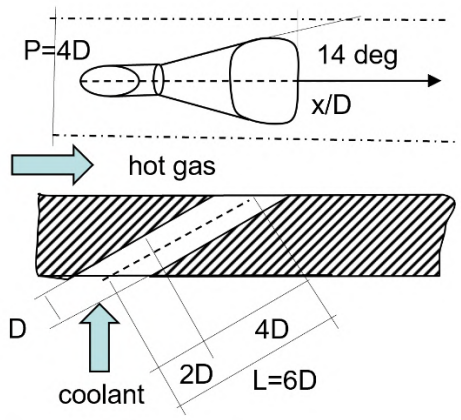


Figure 1: Film cooling baseline geometry based on [7], and baseline for domain 1

Table 1, geometrical parameters, fan shaped hole [7]

| | | **Values** |
|---|---|---|
| D | [mm] | 5 |
| Lateral expansion angle | [deg] | 14 |
| Exit/entry area | [-] | 3.0 |
| Pitch/D | [-] | 4.0 |
| Length/D | [-] | 6.0 |

is modeled as a plenum, but all other parameters remain consistent with the original design [7]. Further details about the experimental setup can be found in [7].
The operating conditions are based on [26].

| | |
|---|---|
| Coolant Temperature | 310K |
| Hot Gas Temperature | 540K |
| Blowing ratio | M=1.2 |
| Turbulence intensity | 3.6% |
| Hot gas Reynolds number | 0.25 $10^5$ |

Table 2, operating parameters, fan shaped hole [26]

This baseline geometry is already optimized and represents a modern turbine film cooling hole design. The geometric specifications, illustrated in Figure 1, include a hole diameter of 5 mm, a lateral expansion angle of 14 degrees, and an outlet width of 30 mm. The area ratio stands at 3.0, the length-to-diameter ratio at 6, and the pitch-to-diameter ratio at 4. The main parameters are repeated and summarized in Table 1.

## 4 Computational domains

Two design domains are used:

- Based on the original work [7] where the code is allowed to modify the shaped hole volume only, no symmetry, figure 2.
- Wider domain, expanding the lateral volume for coolant, symmetry plane, longer main duct 60D, figure 3. The coolant duct is not shaped, it is a prismatic geometry with the same inclination of the original duct.

The computational domain of first configuration is shown in Figure 2 and employs a mesh of 1 million elements. This domain features two inlets, one for the coolant and the other for hot gases. It also incorporates periodic boundary conditions, viscous walls within the coolant duct, and an inviscid condition for the upper wall, **domain 1**. Symmetry plane was not include to investigate if any a-symmetric solution was generated. Figure 3 shows the domain used with the wider rectangular space for the coolant duct, with longer exit used for optimization and for the comparison of the performance of optimal designs, **domain 2.** This second domain as differences, has a larger optimization volume with wider prismatic coolant

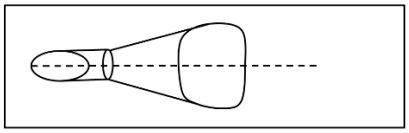

.

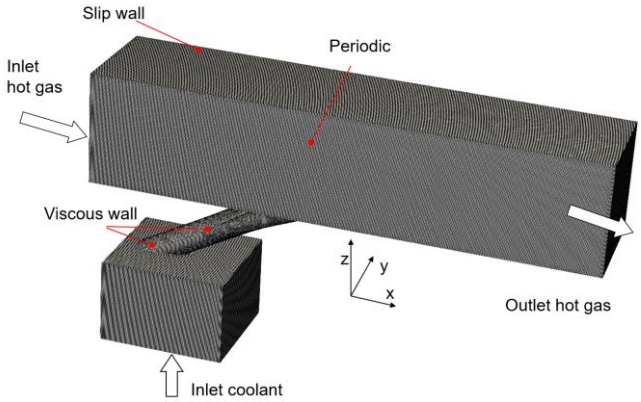


Figure 2: Original duct and computational mesh used for optimization shaped hole, **domain 1**

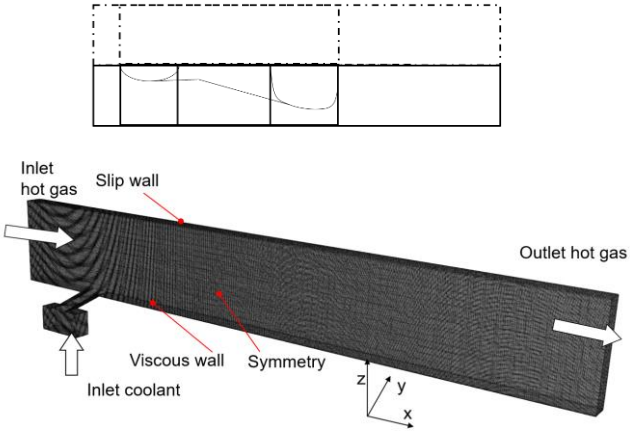


Figure 3: Wider duct geometry and computational mesh used for optimization shaped hole, **domain 2**

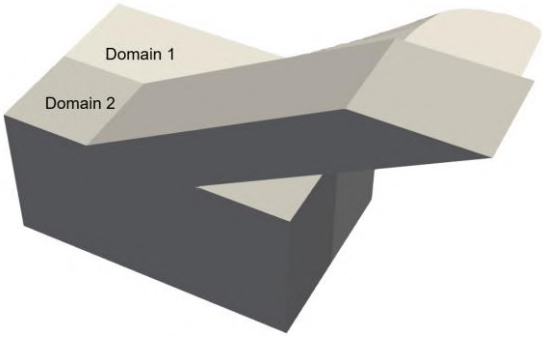


Figure 4: Domain 1 and domain 2 duct detail

duct (figure 4), a symmetry plane, and longer free stream domain (figure 3). All the performance comparisons shown in this paper, are carried out on **domain 2.** The domain is longer because a sensitivity analysis is conducted concerning parameters like inlet and outlet distances, as well as the distance of the inviscid wall from the hole. For this assessment, the outer wall distance from the coolant hole utilized is 60D. For subsequent assessment on domain 2, a grid sensitivity analysis is conducted to discern the impact of mesh resolution on the outcomes and the distance of the boundaries. Three meshes, ranging from 1 million to 6 million elements, are generated, revealing no discernible differences in adiabatic effectiveness beyond 1 million elements. The assessment of performance is based on the same code used before [20-22]. As turbulence closure a k-ω sst formulation is used [23].
The comparison between experiments and CFD simulations of the baseline case [7] are shown in figure 5 on domain 1. The effectiveness is defined as follows:

$$\eta = \frac{T_m - T_{aw}}{T_m - T_c}$$

The x axis shows x/d where zero is located at the downstream edge of the coolant hole. The dots in the graphs are experiments from [7]. The conditions in the experiments differ slightly from the current problem setup – in the original work [7], the coolant duct is not configured as a plenum. The graph shows the adiabatic lateral effectiveness against x/D starting from the downstream edge. The effectiveness is shown for the blowing ratios M=0.5, where the blowing ratio is defined as $M = (\rho_c U_c)/(\rho_m U_m)$. CFD predictions are overpredicting the performance of coolant duct, if compared with experiments. The configuration studied is not exactly the same having no flow in cross flow in the plenum in this case.
While RANS models such as those used in the current work tend to overpredict the adiabatic effectiveness, the overall trend at lower blowing ratio is similar to other observations in literature [7], even if the error increases moving downstream.

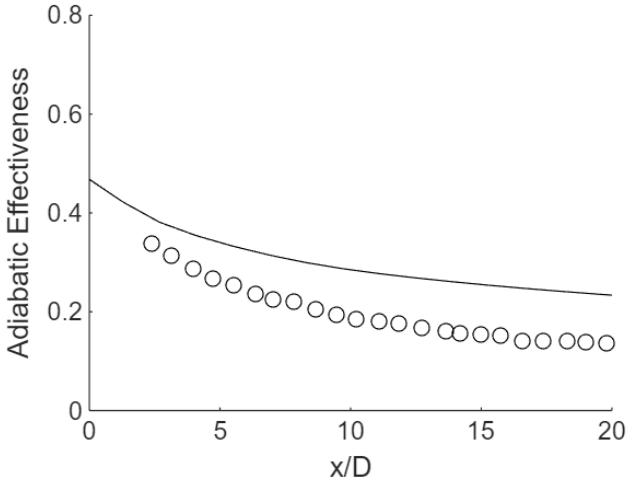


Figure 5: Comparison between CFD and experiments fan shaped hole, M=0.5, TU=3.6% (free stream)

## 5 Optimal geometries for the baseline case, domain 1

Fluid topology optimization for the flow is conducted at a blowing ratio of M=1.2. Figure 6 shows in green the regions where the domain is allowed to change. The maximum variation normal to the wall is 0.2D.
The code can modify the shape of cooled surface to enhance the lateral coverage instead of only changing the shape of coolant hole. In the optimization area the optimizer can add material shaping the hole, the inner duct and the surface upstream and downstream the hole.
As relative weights, the optimizer considers pressure losses f1 and two different thermal conditions: maximum heat transfer on the cooled surface $f_2$ and minimal temperature of the flow volume over the surface, $f_2$ (next paragraph for the wider domain). The objective function to minimize is defined as below, where $f_1$ and $f_2$ are non dimensionalized:

$$F=\omega_1 f_1+\omega_2 f_2 \quad (3)$$

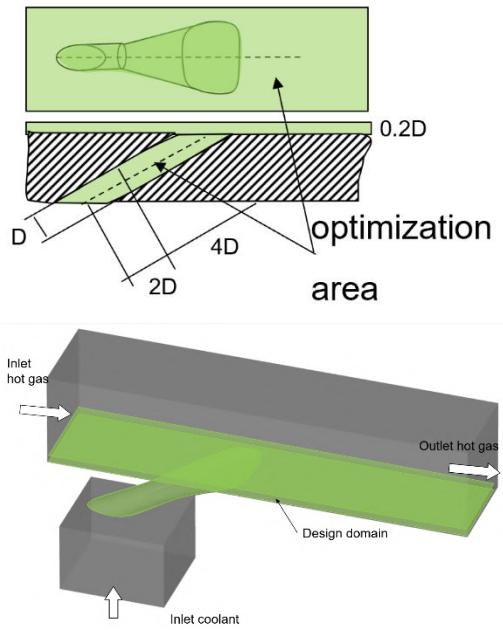


Figure 6: Optimization area, schematic and full 3D volume, domain 1

The resulting optimal geometry is illustrated in Figure 7, where the blue regions represent solid material added by the optimizer to influence the direction of the coolant. Noticeably, there are modifications made within the coolant duct, at the hole exit, and along the cooled surface, both upstream and downstream.
To understand the mechanics of the cooling flow induced by the optimal geometry, a schematic is shown in Figure 7. The optimizer generates a converging ramp upstream of the hole. This geometry pushes the main fluid stream towards the center of the coolant jet, enhancing the lateral spreading. Downstream of this converging structure two dimensional back facing steps anchor the coolant before the coolant hole.
Similar ideas have been proposed in literature by [9-10]. In contrast to what has been shown in literature these structures are converging, pushing the main fluid stream to the central part of the coolant jet. This causes the coolant to spread more

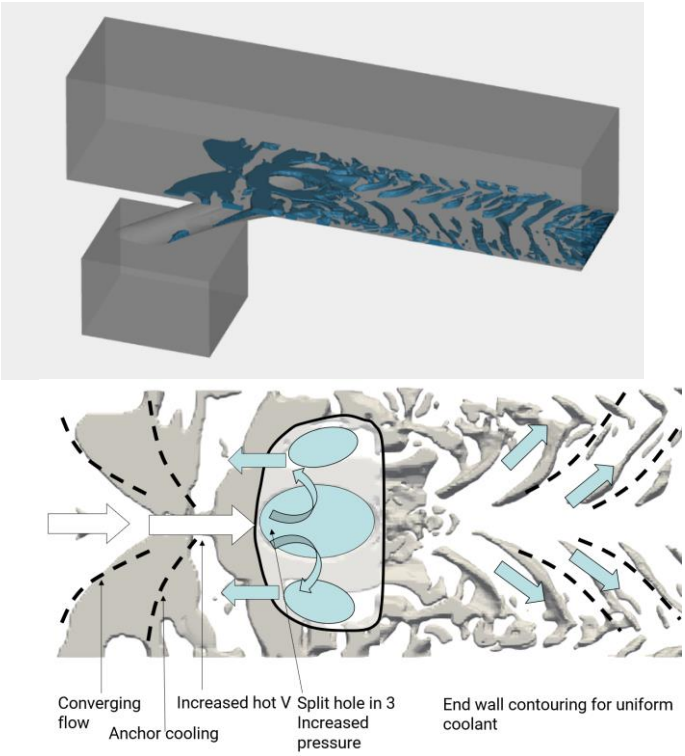


Figure 7. Optimal geometry maximum heat transfer.

laterally, with an effect that resembles cusp design [18]. The combination of upstream geometries, placed at a larger distance from the wall, generates a backward facing step that is anchoring the cooling, even if the complexity is higher than what is usually observed in other designs proposed in the open literature. The optimizer changes the coolant hole structure to a multi-hole configuration instead of a fan-shaped duct.

This is obtained by the optimizer that splits the exit hole in 3, adding material and changing the original shape. This trend has been shown for different optimization parameters and for other geometries not shown in current paper. During the optimization, when the weight of lateral adiabatic effectiveness is increased, a multi-channel configuration appears [11]. Several authors have proposed such configuration with or without a ramp before the hole exit. A three hole design with a shaped dome before the hole has been proposed by Grine et al. [24]. Others have suggested multiple hole distribution without ramp or domes [25]. While what found by the optimizer is not a novelty by itself (as discussed similar geometries for the coolant hole have been proposed), but it is remarkable that the optimizer is able to identify such class of solutions, with no specific user input beyond the requirement to reduce the pressure drop and decrease the surface temperature.

In figure 8 by changing the weighting of equation 3, it is possible to achieve different geometries. Bottom figures it is the case without heat transfer, only to minimize pressure losses $\omega 2=0$. In this case, the optimizer adds material to the channel inlet (where a small recirculation otherwise is observed), in the center of expansion area (where a local separation tends to occur) and on the hole's upstream edge.

While the first two zones are generated to remove the separation region, the third one acts near the upstream edge of the

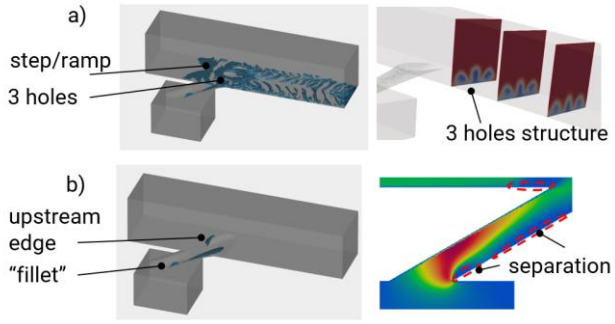


Figure 8 First design suggestions, M=1.2. a) maximum heat transfer, b) no heat transfer target, only pressure losses.

hole exit. This small geometry shields the coolant from the main fluid stream and reduces the shear stress. In figure 8 a) shows what happens when maximum heat transfer is prescribed as objective.

The core concept was that by imposing an isothermal condition on the cooled surface—matching the temperature of the hot gases—heat transfer would reach its maximum in the case of perfect film cooling, where effectiveness equals 1 on the cooled surface. The optimizer leaves the same structures observed in b) but adds a step/ramp in front of the coolant hole, with a converging structure. The hole exit is divided into 3 elliptic holes and downstream splitters are formed, counter acting the vorticity of the kidney vortices. The lateral coverage distribution benefit is shown in figure 9. This is due to the new hole design and to the downstream structures. Downstream of the hole, there is a generation of inclined splitters that have two effects: moving the coolant closer to the wall, generating a region of low pressure, and promoting the lateral coverage of the coolant. Despite some apparent benefits associated with these geometries, there may also be some drawbacks. The splitters locally enhance the heat transfer and in case of poor coolant injection, generates a region with strong heat transfer that is not covered by the coolant.

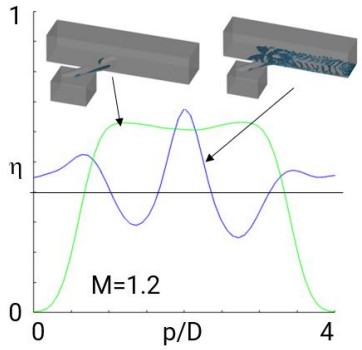


Figure 9 Lateral coverage of adiabatic effectiveness, M=1.2, x/D=4.5

While these splitters downstream the hole are fluid dynamically interesting, the design is not suitable for real applications. The splitters downstream the coolant duct promotes high level of heat transfer and in the case the coolant is not perfectly covering the surface, the turbine surface will suffer damage.

For this reason, the geometry has been simplified, cutting the splitters downstream the coolant as in figure 10. The

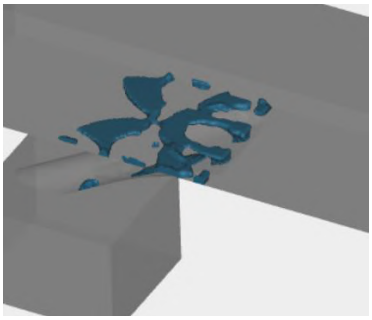

Figure 10 First design suggestions, M=1.2 removing downstream splitters and new optimization, maximum heat transfer. Name: **3 holes cut**

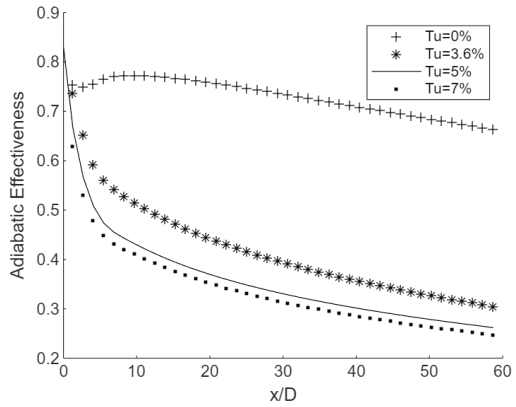


Figure 11 Lateral Adiabatic effectiveness performance with free stream turbulence level, M=1.2, 3 holes cut

performance is overall similar to the most complex design shown before, without having to deal with the risk of splitters after coolant injection. In literature it is found that fan shaped holes are not heavily dependent on free stream turbulence. This does not seem the case for this configuration. CFD predicts some variations of adiabatic effectiveness as function of turbulence, figure 11.

## 6 Wider domain optimization, domain 2

In order to assess the possible capabilities of FTO a wider domain is used as design domain, the **domain 2** already presented. The overall geometry is the same, a coolant duct and an hot gas channel in cross flow. The inclination of the connecting duct, where ToffeeX can generate the new coolant duct is the same of fan shaped hole, but the whole pitch can be used by the code.

The objective function is changed, specifically to minimize the temperature of the coolant downstream the hole ejection up to a distance of 0.2D but the code is not allowed to build any structure downstream the hole injection.

To reduce computing cost, a symmetry plane is used, having half of the pitch of previous case. A 6 million mesh is used for all the cases compared in this paragraph. By changing the relative weight of pressure losses and temperature minimization, several designs can be achieved. In this case two of them are shown.

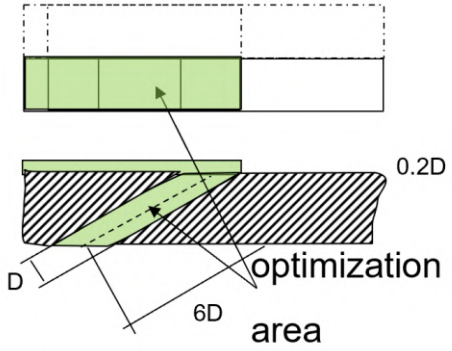


Figure 12: Optimization area, schematic, domain 2

FTO with a wider domain space is showing different coolant duct configurations, as shown in Figure 12. These two configurations are chosen because they show some of the common features found in most of the geometries generated by the solver. While the geometries may be different depending on imposed constraints, there are similarities. In general the solution is a multi hole shape, with multi duct branching inside the duct to feed the multiple ducts (Wide 3). As shown in figure 13 (Wide 4), we observed the generation of large coolant "pockets" inside the coolant duct, feeding the holes. We believe that these pockets may reduce even further the coolant component normal to the surface, increasing the expansion area. The general shape of all structures upstream the duct are similar, with steps and generation of "trench cavities". Another common feature observed is the generation of converging steps in front of coolant ejection. This channels the hot gas against the center of the coolant, promoting a lateral spreading of the coolant. This feature is more clear on the three hole cut configuration but has been found in several designs. The exit hole can go from classical multi-hole configuration to cusp design in many of the configurations generated. The overall performance of the geometries is compared against the default shaped hole in the following graph. The 3 holes cut geometry is re-run on the same computational domain, to have consistent results.

Figure 14, shows the comparison of performance of 3 holes cut, wide 3 and wide 4 against the baseline configuration. Two levels of turbulence have been chosen, Tu=0 and 3.6%.

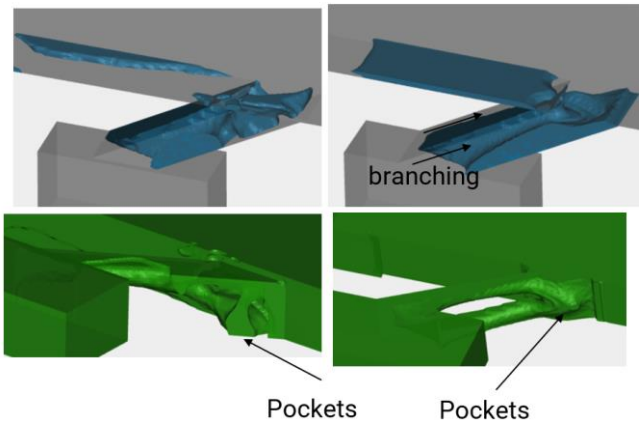


**Wide 3** configuration, solid (top) and fluid (bottom) domain

**Wide 4** configuration, solid (top) and fluid (bottom) domain

Figure 13 Two designs, Wide 3 and Wide 4, by ToffeeX

The results in terms of performance gain are different. There is an advantage of the wide 4 configuration in both cases. For Tu=0% wide 4 has a clear advantage over the baseline of more than 50% until x/D=10. It is shown that the 3 holes cut has very good performance, while wide 3, the less performing configuration in case of Tu=0% has a maximum gain of 20%. For the reference free stream turbulence of 3.6%, the situation changes. Up to x/D=20 the wide 4 geometry is better than the baseline geometry, the 3 holes and wide 3, as laterally averaged adiabatic effectiveness. The 3 holes configuration with the cut, shows a benefit until about x/D=8 for TU=3.6% and marginal impact until x/D=40.

Figure 15 shows a schematic of the exit hole of the configurations studied with symmetry planes for reference. The contour plots in Figure 16 and Figure 17 shows, from top to the bottom, the baseline case, 3 holes cut, wide 3 and wide 4. Wide 3 configuration shows a stripe of less cooled flow in the center of the domain for both Tu=0% and TU=3.6%.

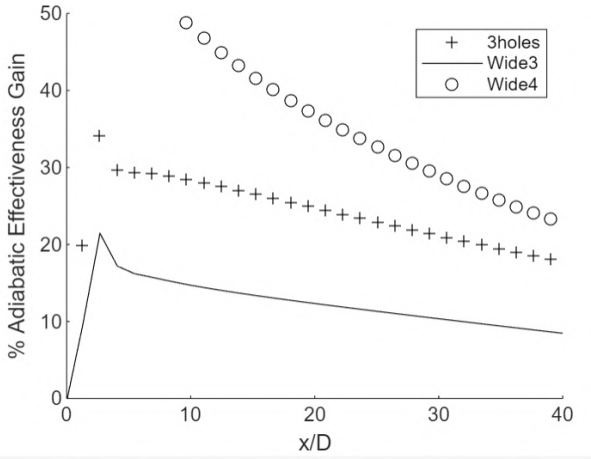


Tu=0%, Adiabatic effectiveness gain

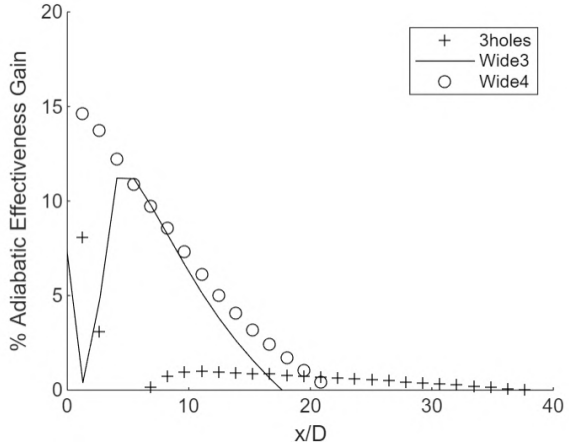


Tu=3.6%, Adiabatic effectiveness gain

Figure 14 Performance gain against baseline for 3 designs, with Tu=0% and Tu=3.6%

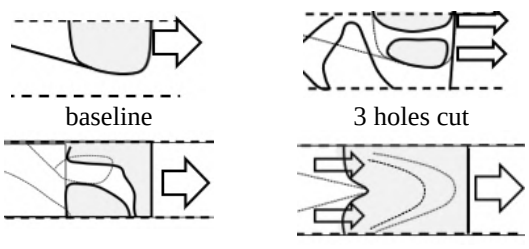


Figure 15 Schematic of exit holes

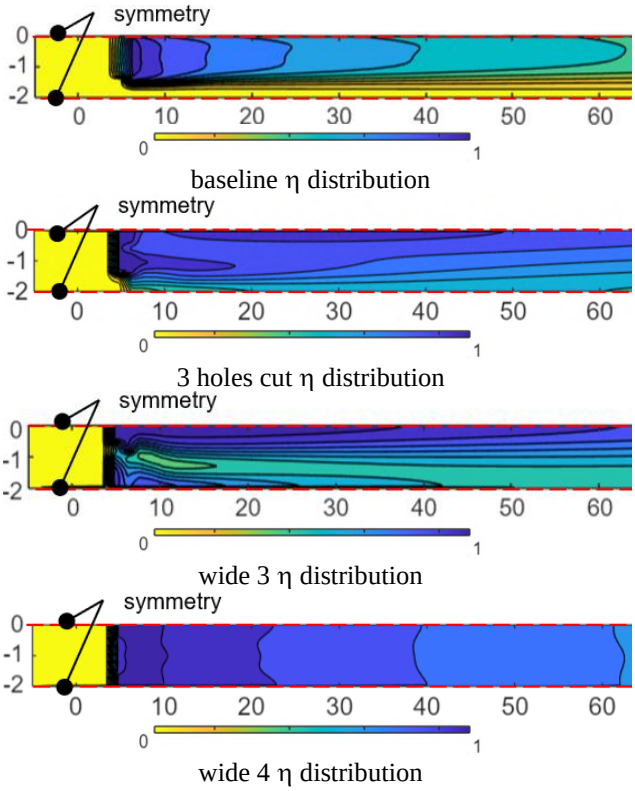


Figure 16 Eta for 4 designs, with Tu=0%, not in scale

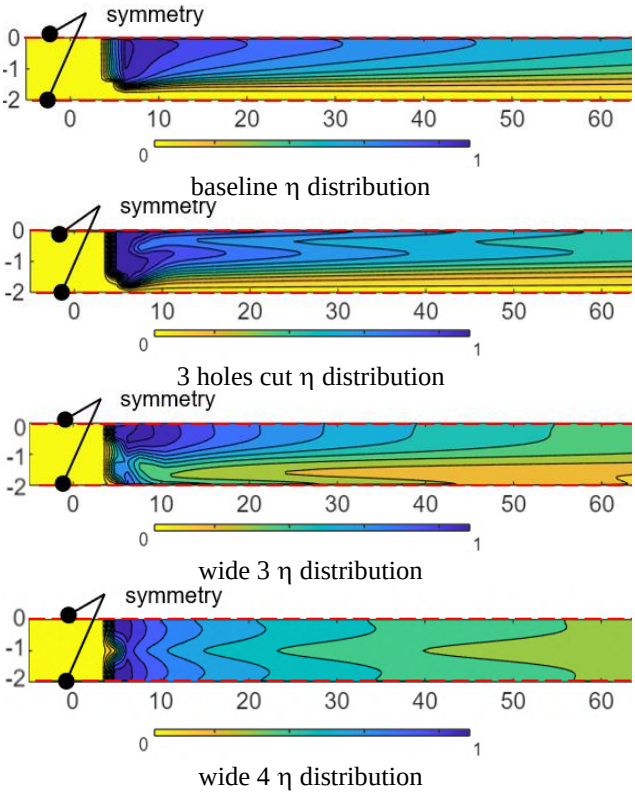


Figure 17 η for 4 designs, with Tu=3.6%, not in scale

Wide 4, among all these configurations shows better performance, having a better lateral coverage. The advantage is maintained even when higher turbulence level is imposed for the main stream. The surface downstream the coolant injection is well covered with wide 4 configuration, from the coolant downstream edge to the exit.

In terms of pressure losses, for 3.6% turbulence, in the 3 holes cut, the overall pressure loss is approximately 1% lower than the baseline default geometry. This is due to a trade off between the beneficial effect of fillet radius at the entrance, and the negative contribution of higher wetted area. In wide 3, the pressure losses are reduced by 22% and 30% for the wide 4 configuration (compared to the baseline). This is due to the higher passing areas obtained during optimization.

# 7 CONCLUSIONS

This work presents a design exploration of fluid topology optimization (FTO) using ToffeeX to film cooling design, with operating conditions representative of those found in gas turbines, while the flat plate is an idealized representation. These ducts can be manufactured using additive manufacturing (or EDM or other laser methods) and their performance is above standard designs.

While the fluid topology optimization solver is not trained in any sense with existing film cooling design, it nevertheless is able to identify features which resemble those proposed in the literature.

In this work two design domains are used for exploration: domain 1, a fan shaped design (an already optimal configuration) and domain 2, a wider design where the code can generate any possible geometry. In both cases, ToffeeX proposes modifications that are improving performance.

In domain 1, to reduce pressure losses the solver modifies the shape of the inner cooling duct and places a geometry in the fan shaped duct. At the same time in many cases, the solver adds a small dome near the upstream edge of the coolant hole to minimize the interaction with hot gases.

To improve adiabatic effectiveness, both in the default fan shaped hole and wider domain, the optimizer generally produces common features:

1. Generation of multiple exits (multiple hole configuration)
2. Adding a converging duct before the coolant hole with some backward facing steps. This is similar to what has been observed by other researchers who have proposed trench cavities, and small ramps in film cooling applications.
3. Complex coolant exits similar to cusp design with deep pockets fed by branching channels.

While experimental validation is needed, the proposed designs show that film cooling of a complete turbine can be also redesigned with this approach.

In particular, by allowing the code a wider design space, the solver is able to generate the so called Wide 4 geometry that has better performance than the baseline case.

# 8 REFERENCES


1. Fadlun E. A., Michelizzi I. De Iaco M. “Measurement error influence on gas turbine operability for condition-based maintenance and reliability/availability improvement”, ASME Turbo Expo 2008, GT2008-50749
2. Goldstein, R., Eckert, E., and Burggraf, F., 1974, “Effects of Hole Geometry and Density on Three-Dimensional Film Cooling,” International Journal of Heat and Mass Transfer
3. Andreopoulos., and Rodi W., 1984, “Experimental Investigation of Jets in a Crossflow,” J. Fluid Mechanics, Vol. 138, pp. 93–127.
4. Papell, S., 1984, "Vortex Generating Flow Passage Design for Increased Film Cooling Effectiveness and Surface Coverage," ASME Paper No. 84-HT-22.
5. Sen, B., Schmidt, D., and Bogard, D., 1996, "Film Cooling With Compound Angle Holes: Heat Transfer", ASME J. of Turbomachinery, Vol. 118, pp. 800–806.
6. Bell, M., Hamakawa, H., Ligrani, P.M., 2000,"Film Cooling From Shaped Holes",ASME J. of Turbomachinery, Vol. 122 pp.224-232
7. Gritsch, M., Saumweber C., Schulz A., Wittig S., Sharp E., 2000 “Effect of internal coolant cross flow orientation on the Cd coefficient of shaped film cooling holes”, J. Turbomachinery Vol. 122
8. Wu, X.; Du, X.; Wang, C. Study on Film Cooling performance of Round Hole Embedded in Different Shaped Craters and Trenches. Aerospace 2021, 8, 147. https://doi.org/10.3390/aerospace8060147
9. Idowu Oguntade, H., E. Andrews, G., Burns, A. D., B. Ingham, D., and Pourkashanian, M. (November 1, 2012). "Improved Trench Film Cooling With Shaped Trench Outlets ." ASME. J. Turbomach. March 2013; 135(2): 021009. https://doi.org/10.1115/1.4006606
10. Montomoli F, A. D’Ammaro, S. Uchida, Numerical and experimental investigation of a new film cooling geometry with high P/D ratio, International Journal of Heat and Mass Transfer, Volume 66, 2013, Pages 366-375
11. Snyder, J. C., and Thole, K. A. (April 30, 2020). "Performance of Public Film Cooling Geometries Produced Through Additive Manufacturing." ASME. J. Turbomach. May 2020; 142(5): 051009. https://doi.org/10.1115/1.4046488
12. Dede, E. M., 2009. “Multiphysics topology optimization of heat transfer and fluid flow systems”. In proceedings of the COMSOL Users Conference, Vol. 715.
13. Dede, E. M., Nomura, T., and Lee, J., 2014. “Multiphysics simulation”. Simulation Foundations, Methods and Applications, Springer London, London.
14. Yoon, G. H., 2010. “Topological design of heat dissipating structure with forced convective heat transfer”. Journal of Mechanical Science and Technology, 24(6), pp. 1225–1233.
15. Matsumori, T., Kondoh, T., Kawamoto, A., and Nomura, T., 2013. “Topology optimization for fluid–thermal interaction problems under constant input power”. Structural and Multidisciplinary Optimization, 47, pp. 571–581.
16. Marck, G., and Privat, Y., 2014. “On some shape and topology optimization problems in conductive and convective heat transfers”. In OPTI 2014, An International Conference on Engineering and Applied Sciences Optimization, pp. 1640–1657.

17. Alexandersen, J., Aage, N., Andreasen, C. S., and Sigmund, O., 2014. “Topology optimisation for natural convection problems”. International Journal for Numerical Methods in Fluids, 76(10), pp. 699–721.
18. Raske, N, Gonzalez, A O, Furino, S, Pietropaoli, M, Shahpar, S, & Montomoli, F. "Thermal Management for Electrification in Aircraft Engines: Optimization of Coolant System." Proceedings of the ASME Turbo Expo 2022: Turbomachinery Technical Conference and Exposition. Volume 6B: Heat Transfer — General Interest/Additive Manufacturing Impacts on Heat Transfer; Internal Air Systems; Internal Cooling. Rotterdam, Netherlands. June 13–17, 2022. V06BT13A013. ASME. https://doi.org/10.1115/GT2022-82538
19. Pietropaoli M., Montomoli F. and Gaymann A., "Three-dimensional fluid topology optimization for heat transfer," Structural and Multidisciplinary Optimization, vol. 59, pp. 801-812, 2019.
20. Casari, N, Di Caterino, A, & Pietropaoli, M. "Topology Optimization of Fuel Cells: an Innovative Approach for Sustainable Aviation." Proceedings of the ASME Turbo Expo 2024: Turbomachinery Technical Conference and Exposition. Volume 5: Cycle Innovations. London, United Kingdom. June 24–28, 2024. V005T06A037
21. Caruso, C, Morante, F, Pampaloni, G, Rossin, S, Canova, A, Casari, N, & Rees, T. "An Additively Manufactured Two-Fluid Heat Exchanger Designed With Topology Optimization Tools." Proceedings of the ASME Turbo Expo 2024: Turbomachinery Technical Conference and Exposition. Volume 13: Heat Transfer: General Interest / Additive Manufacturing Impacts on Heat Transfer; Wind Energy. London, United Kingdom. June 24–28, 2024. V013T13A033. ASME
22. Rees, TW, Azam, A, Casari, N, Banks, P, Jiranek, L, Furino, S, & Muley, A. "An Experimental Case Study in Combining Topology Optimization and Additive Manufacturing Techniques to Generate Novel and High-Performance Compact Heat Exchanger Designs." *Proceedings of the ASME Turbo Expo 2024: Turbomachinery Technical Conference and Exposition*. *Volume 13: Heat Transfer: General Interest / Additive Manufacturing Impacts on Heat Transfer; Wind Energy*. London, United Kingdom. June 24–28, 2024. V013T13A040. ASME.
23. Wilcox D. C., Turbulence modeling for CFD, La Canada: DWC Industries, Inc. 1993.
24. Grine, M., Boualem, K., Dellil, A.Z. et al. Improving adiabatic film-cooling effectiveness spanwise and lateral directions by combining BDSR and anti-vortex designs. Thermophys. Aeromech. 27, 749–758 (2020). https://doi.org/10.1134/S0869864320050091
25. Fan Yang, Mohammad E. Taslim, "Experimental Film Cooling Effectiveness of Three-Hole-Branch Circular Holes", International Journal of Rotating Machinery, vol. 2021, Article ID 6691128, 19 pages, 2021. https://doi.org/10.1155/2021/6691128
26. Saumweber, C., Schulz , A., and Wittig, S. (January 23, 2003). "Free-Stream Turbulence Effects on Film Cooling With Shaped Holes ." ASME. *J. Turbomach*. January 2003; 125(1): 65–73. https://doi.org/10.1115/1.1515336